

11. N. F. Kashapov and A. M. Minnigulov, in: *Gas Discharge Physics* [in Russian], Kazan' (1988), pp. 17-24.
12. G. V. Gembarzhevskii and I. A. Generalov, *Teplofiz. Vys. Temp.*, **24**, No. 2, 233-238 (1986).
13. G. G. Arutyunyan and G. A. Galechyan, *Zh. Tekh. Fiz.*, **48**, No. 3, 831-834 (1978).

## RADIAL DISTRIBUTION OF ELECTRON CONCENTRATION IN A COMPRESSED LAYER

I. A. Anoshko, V. S. Ermachenko, and L. E. Sandrigailo

UDC 533.9.082

*We present results obtained in the measurement of electron concentrations in compressed layers, derived in the plasma deceleration of an end-face Hall accelerator with a flat solid barrier, and these measurement results were then compared with analogous measurement results obtained in free flows.*

The study of the parameters in plasma jets has been stimulated by their extensive utilization in a number of branches of science and engineering [1, 2]. The present study continues the investigation to determine the parameters of a plasma generated by an end-face Hall accelerator (EHA) [3-5]. In [5] we find an experimental determination of the electron concentration in free plasma flows. At the same time, in the streamlining of the barrier by hypersonic plasma flows a deceleration zone is established, where the plasma parameters are significantly different from the corresponding parameters in a free jet, a fact which must necessarily be taken into consideration in evaluating the action of a plasma flow onto the surface of a solid. In this connection, results from such investigations are of particular interest. The process of gas-jet deceleration has been studied rather fully [6, 7], and it may serve as a characteristic as well for weakly ionized plasma flows. However, there exists virtually no theoretical and experimental studies into the processes of interaction with solid barriers on the part of plasma jets exhibiting a high level of ionization.

Here we have studied transverse luminescence spectra and we have determined the electron concentrations in compressed layers. For the purposes of this investigation, we chose EHA operating regimes in which measurements similar to those in a free jet were conducted: the magnetic-field induction  $B = 1$  T in the discharge zone, the discharge current  $J = 2200, 2600,$  and  $3000$  A, the working gas flow rate  $G_{\Sigma} = 10$  g/sec (8.5 g for air and 1.5 g for nitrogen), and the vacuum-chamber pressure  $P_{ch} = 1.2 \cdot 10^3$  Pa. Here the velocity of the plasma was approximately 10-15 km/sec. This velocity was determined from pressures measured in the operating sections of the flow by means of a combined Pitot-Prandtl fitting, and from the deceleration enthalpy.

To produce a compressed layer along the path of the plasma jet a flat barrier fabricated in the form of a hollow copper cylinder with a diameter of 120 mm was set up perpendicular to the axis of the jet. The axis of the cylinder coincided with the axis of the flow. The barrier was cooled by pumping water through the inside cavity of the cylinder. The barrier diameter was chosen on the basis of jet dimensions. The barrier was positioned at a distance of  $L = 140$  and  $170$  mm from the outlet of the accelerator nozzle. Depending on the discharge current and the working cross section, the thickness of the compressed layer was varied within limits of 25-30 mm. The radiation spectra for the compressed layer were recorded at sections removed from the plane of the barrier surface through a distance of 10 mm. One such photograph of the compressed layer is shown in Fig. 1.

A spectroscopic analysis of the plasma composition demonstrated that the radiation spectrum is sensitive to the magnitude of the energy introduced into the discharge, but the qualitative composition of the spectra remains unchanged both for the free jet and for the compressed layer. We should take note, however, that the intensity of radiation for the spectral lines of the compressed layer exceeds by factors of 15-20 the corresponding values for the free jet.

The luminescence spectra for the compressed layer in the 430-580 nm wavelength band consists primarily of isolated lines of NI and NII nitrogen atoms and ions. None of the lines for the elements contained in the composition of the barrier were seen. The hydrogen line  $H_{\beta}$  is observed in each of the cases, and its presence is probably associated with the existence of a small admixture of water vapors in the supply system (Fig. 2). It is noticeably broadened on the spectrum of the compressed layer. In order to determine the electron concentrations we employed a method based on the broadening of the  $H_{\beta}$  line as a consequence of the

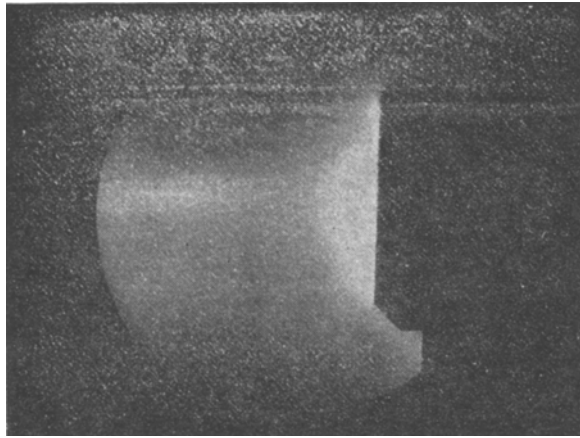


Fig. 1. Photograph of compressed layer.

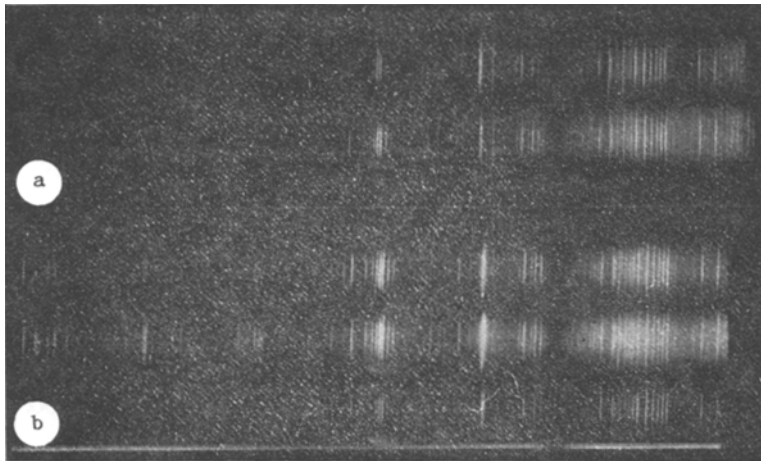


Fig. 2. Radiation spectra: a) free jet; b) compressed layer;  $L = 160$  mm,  $J = 2200$  A.

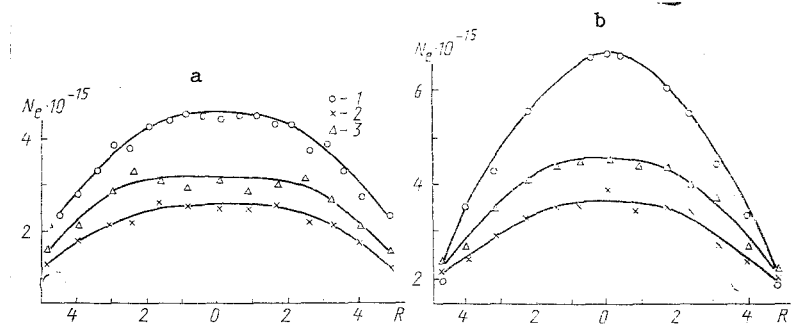


Fig. 3. Radial distribution of electron concentration in compressed layer,  $L = 130$  (a) and  $160$  mm (b): 1)  $J = 2200$  A; 2)  $2600$ ; 3)  $3000$ .

linear Stark effect. The method of determining the radial broadening of the  $H_{\beta}$  line from transverse emission spectra for the plasma being studied here has been described in detail in [5]. In calculations of the Stark broadening of the  $H_{\beta}$  line we have taken into consideration the operational function of the spectrographic equipment.

Figure 3 shows graphs of the radial distribution of electron concentration in the compressed layer, as functions of the strength of the discharge current and the distance from the outlet of the accelerator nozzle. It follows from an analysis of these graphs that there exists within the central portion of the compressed layer a region with a virtually constant electron concentration through the cross section, whose dimension we will denote as  $R_c$ . The noticeable growth of this region is found to occur as the strength of the discharge current is increased and as the distance from the nozzle outlet is reduced. A similar quantitative relationship between the change in  $R_c$  and the rise in the strength of the current is found to occur also in a free plasma jet [5]. It follows from an analysis of graphs (Fig. 3a, b) of corresponding identical values for the strength of the discharge current that the distance of the compressed layer from the nozzle outlet at  $J = 2600$  and  $3000$  A does not significantly affect the nature of the radial electron distribution, and its near-axial values differ from one another virtually within the limits of the measurement error, which amounts to 15-20%. The greatest difference in the corresponding curves is observed for  $J = 2200$  A, with the electron concentration at the center of the compressed layer noticeably higher with increasing distance from the nozzle outlet. For each individual separate position of the barrier this growth in the strength of the discharge current leads to reduction and subsequent constancy of concentration within the central portion of the compressed layer.

A different relationship between the axial values for electron concentration and the strength of the discharge current is observed in a free plasma jet. It has been established experimentally that at distance of  $L = 130$  mm the concentration of electrons at the center of a plasma jet increases as the current strength is increased [5]. Similar electron-concentration values for  $L = 160$  mm were determined from the broadening of the  $H_{\beta}$  line found from the total distribution of its radiation intensity in a direction perpendicular to the axis of the plasma flow. It turned out that the axial values for electron concentration at  $L = 160$  mm change within limits of  $5 \cdot 10^{14}$  to  $8 \cdot 10^{14}$   $\text{cm}^{-3}$  as the discharge current increases from 2200 to 3000 A. The error in the determination of the concentration in this case has been estimated at 30-40%. It follows out of a comparison of the results derived here and the data in [5] that with increasing distance from the outlet of the accelerator nozzle the axial values of electron concentration in a free jet become smaller by factors of 2 to 3, while the tendency of these values to increase is simultaneously retained as the strength of the discharge current is increased.

The electron concentration at the center of the compressed layer is noticeably increased in comparison to analogous values for  $N_e$  in the free jet. Thus, with a barrier distance of  $L = 170$  mm the electron concentration at the center of the compressed layer increases by a factor of 15 when  $J = 2200$  A and by a factor of 5-6 when  $J = 2600$  and  $3000$  A. As the barrier approaches the nozzle outlet ( $L = 140$  mm) the electron concentration in the compressed layer increases by a factor of 2-3 in comparison to a free jet. As follows from a comparison of the experimental data in the compressed layer (Fig. 3) and in the free jet [5], the sharp rise in concentration at the center of the compressed layer is found to occur when the plasma jet with a sharp maximum in radial distribution  $N_e(r)$  impinges on the barrier. When a jet with a plane apex in the profile of  $N_e(r)$  impinges on the barrier, the electron concentration in the compressed layer increases to a smaller degree.

Thus, analysis of the derived results allows us to draw the conclusion that the decisive effect on the distribution of  $N_e(r)$  in the compressed layer is exerted by the profile of the function  $N_e(r)$  for the jet incident on the barrier. The profile of  $N_e(r)$  is, in turn, associated with the dimensions of the region of virtually unchanged electron concentration  $R_c$  and possibly with the concentrations of other plasma components. The mutual relationship between  $R_c$  and the diameter  $D$  of the cylindrical barrier determines the observed effects in the compressed layer: when  $R_c \ll D$  the influence of the plasma stream on the parameters in the compressed layer is at its greatest; as the ratio  $R_c/D$  increases, the increase in electron concentration and in its gradient of change diminishes, and then ceases entirely. Moreover, in analogy with a gas jet [8] one might assume that the absence of maxima in electron distribution (nonaxial) in the compressed layer is governed by radial leakage of the plasma jet at the barrier.

#### NOTATION

$J$ , discharge current, A;  $G_{\Sigma}$ , working gas flow rate, g/sec;  $B$ , magnetic field induction, T;  $P_c$ , vacuum chamber pressure, Pa;  $L$ , distance from the nozzle outlet of the accelerator, mm;  $R$ , radius, cm/  $N_e$ , electron concentration,  $\text{cm}^{-3}$ ;  $H_{\beta}$ , Balmer hydrogen line with a wavelength of 486.1 nm;  $R_c$ , dimension of region with constant electron concentration;  $D$ , barrier diameter. Subscripts:  $\Sigma$ , total working gas flow rate; e, electron component; ch, chamber conditions; c, constant-value condition.

#### LITERATURE CITED

1. L. A. Artsimovich (ed.), *Plasma Accelerators* [in Russian], Moscow (1972).

2. S. D. Grishin, L. V. Leskov, and N. P. Kozlov, *Electric Rocket Engines* [in Russian], Moscow (1975).
3. V. S. Ermachenko, F. B. Yurevich, M. N. Rolin, et al., *Inzh.-Fiz. Zh.*, **35**, No. 3, 459-465 (1978).
4. I. A. Anoshko, F. B. Yurevich, V. S. Ermachenko, et al., *Zh. Prikl. Spektrosk.*, **40**, No. 5, 926-931 (1984).
5. I. A. Anoshko, V. S. Ermachenko, M. N. Rolin, et al., *Inzh.-Fiz. Zh.*, **57**, No. 3, 491-493 (1989).
6. B. G. Semiletko and V. N. Uskov, *Inzh.-Fiz. Zh.*, **23**, No. 3, 453-459 (1972).
7. E. I. Sokolov, A. V. Startsev, V. N. Uskov, et al., *Inzh.-Fiz. Zh.*, **32**, No. 2, 247-250 (1977).
8. E. I. Sokolov and I. V. Shatolov, *Izv. Akad. Nauk SSSR, Mekh. Zhidk. Gaza*, No. 3, 47-52 (1983).

**THERMAL PROPERTIES OF SUPERHEATED POTASSIUM VAPOR AT TEMPERATURES UP TO 2150 K AND PRESSURES UP TO 10 MPa.**

**2. DEVELOPMENT OF THERMODYNAMIC FUNCTION TABLES**

N. G. Vargaftik, A. N. Nikitin, V. G. Stepanov,  
and A. I. Abakumov

UDC 546.32:533.11+536.411

*Based on experimental data on thermal properties, we have constructed tables of thermodynamic functions for superheated potassium vapor, and these include the values of the specific volume  $v$ , enthalpy  $h$ , entropy  $s$ , isobaric  $C_p$  and isochronous  $C_v$  heat capacities, speed of sound  $A$ , coefficient of compressibility  $Z$ , and they encompass areas of parameters related to pressure  $P = 0.1-10.0$  MPa and temperature  $T = 1075-2150$  K.*

In order to calculate the tables of thermodynamic functions, we used a method proposed in [1-3], which had been used successfully by the authors to describe the properties of a number of gases. In accordance with this method, to generalize the experimental data of the PvT relationships of the potassium gas phase we chose an empirical equation of state of the following form:

$$Z = 1 + \sum_{i=1}^{\alpha} \sum_{j=0}^{\gamma} b_{ij} \frac{\omega^i}{\tau^j}, \quad (1)$$

which may formally be interpreted as a portion of the known virial expansion [4], where  $\omega = \rho/\rho_{cr}$  and  $\tau = T/T_{cr}$  respectively represent the critical points of density and temperature, referred to the parameters. The constants  $b_{ij}$  were determined by the method of least squares. The linear system of normal equations derived out of the conditions of the minimum quadratic functional was solved by the method of singular expansion. The set of thermal-property data provided the basis for the construction of a set of

TABLE 1. Coefficients  $b_{ij}$  for Equation of State (1)

$i$	$j$				
	1	2	3	4	5
0	-0,67220	1,85940	-0,60309	-0,23054	-0,052217
1	-0,89153	1,83340	-0,77899	-0,27837	-0,061728
2	-0,26319	1,78050	-0,98964	-0,33459	-0,072810
3	0,08680	1,68850	-1,2422	-0,40079	-0,085726
4	0,08753	1,54090	-1,5461	-0,47882	-0,10079
5	-0,19345	1,32130	-1,9130	-0,57096	-0,11839
6	-0,46735	1,02000	-2,3582	-0,67999	-0,13895
7	-0,26365	0,65103	-2,9009	-0,80938	-0,16303
8	0,55070	0,28305	-3,5653	-0,96342	-0,19126
9	-0,17398	0,09825	-4,3819	-1,14750	-0,22444